Forensic Analysis of JPEG-Domain Enhanced Images via Coefficient Likelihood Modeling

Jianquan Yang, Guopu Zhu, *Senior Member, IEEE*, Yao Luo, Sam Kwong, *Fellow, IEEE*, Xinpeng Zhang, *Member, IEEE*, and Yicong Zhou, *Senior Member, IEEE*

***Abstract*— JPEG-domain enhancement improves the visual quality of JPEG images by directly manipulating the decoded DCT (discrete cosine transform) coefficients, which inevitably leads to mixed compression and enhancement artifacts. Existing forensic methods that merely consider JPEG artifacts are unsuitable to address such mixed artifacts and hence suffer a considerable performance decline in compression parameter estimation and lack the ability to estimate the enhancement parameter. This work attempts to explore the characterization of the mixed artifacts, and to further estimate both the enhancement and compression parameters of JPEG-domain enhanced images. First, a statistical likelihood function is proposed to characterize the periodicity of DCT coefficients, which can measure how well an enhanced image is de-enhanced back to its JPEG compressed version given the compression and enhancement parameters. The proposed likelihood function reaches its maximum if the parameters match their true values. Then, a forensic method of enhancement detection and parameter estimation is developed based on the proposed likelihood function for two kinds of classical JPEG-domain enhancement. Specifically, JPEG-domain enhanced images are detected by thresholding a scalar feature computed upon the likelihoods, and the enhancement and compression parameters are estimated by locating the maximal likelihood. In addition, mathematical proof of the de-enhancement feasibility is provided. Experimental results demonstrate that the proposed method outperforms the compared methods in both enhancement detection and parameter estimation.**

***Index Terms*— Image forensics, coefficient periodicity analysis, JPEG-domain enhancement, maximum likelihood estimation, quantization step estimation.**

Manuscript received December 26, 2020; revised March 8, 2021; accepted March 29, 2021. Date of publication April 5, 2021; date of current version March 9, 2022. This work was supported in part by the National Natural Science Foundation of China under Grant 61802382, Grant 61872350, Grant U1936214, and Grant 61572489; in part by the Hong Kong GRF-RGC General Research Fund under Grant 9042816 (CityU 11209819) and Grant 9042958 (CityU 11203820); in part by the Science and Technology Development Fund, Macau, under Grant 189/2017/A3; in part by the University of Macau under Grant MYRG2018-00136-FST; in part by the Tip-top Scientific and Technical Innovative Youth Talents of Guangdong Special Support Program under Grant 2019TQ05X696; in part by the Guangdong Basic and Applied Basic Research Foundation under Grant 2020A1515010640; and in part by the Basic Research Program of Shenzhen under Grant JCYJ20170818163403748. This article was recommended by Associate Editor J.-M. Guo. *(Corresponding author: Guopu Zhu.)*

Jianquan Yang is with the Shenzhen Institute of Advanced Technology, Chinese Academy of Sciences, Shenzhen 518055, China, and also with the Shenzhen College of Advanced Technology, University of Chinese Academy of Sciences, Shenzhen 518055, China (e-mail: jq.yang@siat.ac.cn).

Guopu Zhu is with the Shenzhen Institute of Advanced Technology, Chinese Academy of Sciences, Shenzhen 518055, China (e-mail: gp.zhu@siat.ac.cn).

Yao Luo was with the Shenzhen Institute of Advanced Technology, Chinese Academy of Sciences, Shenzhen 518055, China. She is now with Accuray Inc., Chengdu 610000, China (e-mail: yaoluo-ynu@hotmail.com).

Sam Kwong is with the Department of Computer Science, City University of Hong Kong, Hong Kong, and also with the City University of Hong Kong Shenzhen Research Institute, Shenzhen 518000, China (e-mail: cssamk@cityu.edu.hk).

Xinpeng Zhang is with the School of Computer Science, Fudan University, Shanghai 200433, China (e-mail: zhangxinpeng@fudan.edu.cn).

Yicong Zhou is with the Department of Computer and Information Science, University of Macau, Taipa 999078, Macau (e-mail: yicongzhou@um.edu.mo).

Color versions of one or more figures in this article are available at https://doi.org/10.1109/TCSVT.2021.3071218.

Digital Object Identifier 10.1109/TCSVT.2021.3071218

I. Introduction

RECENT years have witnessed massive growth in the volume of digital images due to the prevalence of acquisition devices and social networks. In the meantime, the increasing availability of sophisticated editing software has enabled us to retouch or alter an image without leaving notable visual traces. Such manipulated images in near-photographic quality can be used for malicious intent such as discrediting government authority, misleading public opinion or disparaging personal reputation. As a promising technology for authenticating the trustworthiness of digital images, image forensics [1], [2] has achieved substantial progress over the past decades.

One of the main tasks in image forensics is to detect whether an image has been processed by a given operation and further estimate the used parameter if possible. In the literature, considerable attention has been paid to the forensic analysis of resampled images [3]–[5], filtered images [6], [7], sharpened images [8], geometrically transformed images [9], seam carved images [10], inpainted images [11], and etc. With the popularization of JPEG compression, considerable effort has been devoted to the forensic analysis of images that have undergone JPEG compression once [12]–[20], twice [21]–[24] or multiple times [25]–[27].

This paper focuses on the forensic analysis of images that have undergone JPEG-domain enhancement. As the name implies, JPEG-domain enhancement is specially devised to enhance a JPEG image by directly manipulating its discrete cosine transform (DCT) coefficients so that the manipulated coefficients can yield a pixel matrix with improved contrast. This manner of enhancement can leverage the coefficient sparsity and frequency structures naturally available in a JPEG image, which brings some advantages such as low computational cost and good adaptability to the frequency response of the human visual system. In the literature, numerous works have focused on proposing diverse methods [28]–[33] for

JPEG-domain enhancement; however, little attention has been paid to the forensic analysis of JPEG-domain enhancement.

Forensic analysis of JPEG-domain enhancement includes two aspects: enhancement detection and parameter estimation. Enhancement detection is to detect whether a given image has been enhanced by a specific JPEG-domain enhancement method, and parameter estimation is to estimate both the enhancement and compression parameters of a detected enhanced image. Addressing these forensic concerns is of great interest to many applications [1], [2]. Taking tampering localization as an example, by detecting the presence of enhancement and estimating the used parameters block by block over a suspected image, any inconsistency in either the detected or estimated results can be visualized to reveal the possible tampered region(s). In general, parameter estimation is a task more difficult than enhancement detection, as shown in Section IV. Therefore, the following pays more attention to the parameter estimation of JPEG-domain enhancement.

A JPEG-domain enhanced image is an image (pixel matrix) that has undergone JPEG compression followed by JPEG-domain enhancement, of which both the compression and enhancement parameters are unknown and need to be estimated. The enhancement operation introduces enhancement artifacts that disturb the intrinsic JPEG artifacts, causing both artifacts to be mixed. A straightforward strategy to analyze such mixed artifacts is to regard enhancement artifacts as a kind of noise, so a JPEG-domain enhanced image can be regarded as a JPEG decompressed image contaminated with enhancement artifacts. This strategy suggests that it seems feasible to estimate the compression parameter of JPEG-domain enhanced images by directly using the existing methods originally designed for JPEG decompressed images [12]–[20], despite neglecting the estimation of the enhancement parameter. However, in practice, the influence of enhancement artifacts is far beyond the resistibility of the existing methods, making their performance decline dramatically when dealing with JPEG-domain enhanced images, as will be reported in Section V. Moreover, the existing methods lack the ability to estimate the enhancement parameter.

In this work, we explore the characterization of the mixed artifacts, and make a preliminary attempt to detect JPEG-domain enhanced images and estimate their parameters. Some beneficial results are achieved in this unaddressed direction in image forensics. The main contributions are summarized as follows.

- A generic likelihood function with respect to the enhancement and compression parameters is proposed to characterize the periodicity of coefficients de-enhanced from a JPEG-domain enhanced image. The proposed function reaches its maximum if its parameters match the true values. This property is the key to the forensic analysis of JPEG-domain enhancement.
- A forensic method is developed based on the proposed likelihood function for two classical JPEG-domain enhancement methods (one is non-recursive and the other is recursive). The de-enhancement feasibility of these two enhancement methods is also mathematically analyzed. The presence of enhancement is detected by thresholding a scalar feature computed upon the likelihoods, while the enhancement and compression parameters are estimated by locating the maximal likelihood.
- Experimental results under various settings are provided to validate the effectiveness of the proposed forensic method in both enhancement detection and parameter estimation, demonstrating its superiority over the compared methods.

The rest of the paper is structured as follows. Section II briefly reviews the related works. Section III elaborates on the proposed likelihood function, and Section IV details the developed forensic method for two classical methods of JPEG-domain enhancement. Experimental results are reported and discussed in Section V, followed by conclusions drawn in Section VI.

II. Related Work

In this section, we briefly review related works on two aspects: 1) JPEG-domain enhancement and 2) quantization step estimation of JPEG decompressed images.

A. JPEG-Domain Enhancement

JPEG-domain enhancement emerged almost as early as the release of JPEG compression. Aghagolzadeh *et al.* [28] proposed alpha-rooting to enhance JPEG image contrast by raising the DCT coefficient magnitude to a power alpha, while keeping the coefficient sign unchanged. Konstantinides *et al.* [29] proposed to sharpen a JPEG image by scaling its quantization table with a matrix of scaling factors, at the cost of only 64 additional multiplications regardless of image resolution. Unlike the former two methods that performed enhancement without explicitly defining a contrast measure, Tang *et al.* [30] first defined a contrast measure in a band-wise manner and then used it to control the strength of quantization table scaling. Another band-wise contrast measure was proposed in [31], which was further employed to develop a recursive method that can achieve primitive multi-scale enhancement. Lee [32] separated each DCT coefficient into two components (namely illumination and reflectance) based on the retinex theory, subsequently modified them in different ways and finally perform element-wise product of the two modified components to yield the enhanced coefficient. Mukherjee and Mitra [33] proposed to enhance color JPEG images by nonlinearly mapping DCT coefficients while avoiding pixel value overflow and color distortion. A variant of the previous enhancement method was proposed in [34]. The common advantages shared by these representative methods of JPEG-domain enhancement are their relatively low computational cost and storage requirement, which make them suitable for resource-constrained scenarios. With recent progress in DCT acceleration and optimization [35]–[37], JPEG-domain enhancement as well as other JPEG-domain operations [38]–[40] can be implemented with much higher efficiency.

B. Quantization Step Estimation of JPEG Decompressed Images

A number of works [12]–[20] has contributed to estimating the quantization steps of JPEG decompressed images,

which are unavailable after decompression but useful in many applications such as blocking removal and forgery detection. Fridrich *et al.* [12] proposed a "compatibility" function to measure the degree of a tested step as the true step, and the one with best "compatibility" was taken as the step estimate. Fan *et al.* [13] devised a likelihood model by assuming a Laplacian distribution on raw DCT coefficients and yielded the step estimate based on maximum likelihood principle. Neelamani *et al.* [14] extended the method [13] to color images by further considering the influence of color space transform and interpolation. After observing the relationship between the quantization step and the periodicity of the coefficient distribution, Ye *et al.* [15] proposed a simple yet effective estimation method by counting the local peaks in the power spectrum of the coefficient histogram. Lin *et al.* [17] improved upon the method [15] by classifying the energy density spectra of coefficient histograms into four types and designing estimation rules for each type. A mathematical analysis of JPEG errors was conducted by Luo *et al.* in [16], where the authors also demonstrated the applications of the error analysis to detect decompressed bitmaps and estimate the quantization steps. Li *et al.* [18] deepened the analysis of JPEG errors in consecutive compression and proposed a statistic-sufficient estimator to overcome the technical defects of [12]. Recently, Thai *et al.* [19] proposed a sophisticated method for step estimation by modeling the quantized alternating current (AC) DCT coefficient under the assumption of a doubly stochastic distribution instead of a Laplacian [13], [16], [18] or truncated Gaussian [14] distribution. Yang *et al.* [20] proposed a clustering-based framework to alleviate the insufficiency of coefficients by collecting as many coefficients as possible before step estimation, which helps to improve the estimation performance of the existing methods, especially for small-size images.

These forensic methods were originally proposed for JPEG decompressed images, which merely considered compression artifacts. Directly applying these methods to address JPEG-domain enhanced images will lead to two limitations. First, they suffer a performance decline in compression parameter estimation due to their weak resistibility against the interference caused by enhancement artifacts. Second, they lack the ability to estimate the enhancement parameter.

III. Proposed Likelihood Function

This section first presents the basic idea for characterizing the mixed artifacts caused by JPEG-domain enhancement, then derives the de-enhanced coefficient distribution for likelihood modeling, and finally details the construction of the proposed likelihood function. The main notations used in this section are summarized in Table I.

TABLE I
NOTATIONS

$\mathbf{C}$	Unquantized DCT coefficient matrix
$\mathbf{D}$	Dequantized DCT coefficient matrix
c_{ij}^k	Element of $\mathbf{C}$ at frequency (i,j) of the k-th block
d_{ij}^k	Element of $\mathbf{D}$ at frequency (i,j) of the k-th block
q_{ij}	Quantization step for frequency (i,j)
λ	Enhancement parameter
$\lambda^\star$	True value of λ
$f(\cdot)$	Enhancement operator
$f^{-1}(\cdot)$	De-enhancement operator
$\bar{\mathbf{D}}$	Enhanced DCT coefficient matrix
$\mathbf{D}(\lambda)$	DCT coefficient matrix de-enhanced by λ
$\mathbf{D}^\star$	DCT coefficient matrix de-enhanced by $\lambda^\star$
$d_{ij}^k(\lambda)$	Element of $\mathbf{D}(\lambda)$ at (i,j) of the k-th block
$d_{ij}^\star$	Element of $\mathbf{D}^\star$ at frequency (i,j)
$P_L(\cdot)$	Quantized Laplacian probability mass function
$G(\cdot)$	Truncated Gaussian probability density function

A. Basic Idea

The procedure of (lossy) JPEG compression consists of three main operations, namely block-wise DCT, coefficient quantization and entropy encoding, where coefficient quantization serves to approximate continuous coefficients with discrete ones to reduce the bits required. Let $\mathbf{C}$ and $\mathbf{D}$ denote the whole coefficient matrixes before and after quantization. The elements of $\mathbf{C}$ and $\mathbf{D}$ at the spatial frequency (i, j) of the k-th 8×8 DCT block are respectively denoted by c_{ij}^k and d_{ij}^k, $0 \le i, j \le 7$. Quantization is an element-wise operation that can be formulated by

$$d_{ij}^k = \text{round}\left(\frac{c_{ij}^k}{q_{ij}}\right) * q_{ij}, \tag{1}$$

with round$(\cdot)$ the rounding operator and q_{ij} the quantization step. Unless necessary, the block index k is omitted for simplicity.

The quantized coefficient matrix $\mathbf{D}$ has several attractive properties for image enhancement. First, $\mathbf{D}$ represents an image from the frequency perspective, which provides a convenient way to adapt the frequency response characteristics of the human visual system. Second, $\mathbf{D}$ is commonly sparser (i.e., has more zero-valued coefficients) than $\mathbf{C}$, which provides a possibility to reduce the computational cost of enhancement.

To take advantage of these properties, JPEG-domain enhancement directly manipulates the coefficients $\mathbf{D}$ of a JPEG image and then inversely transforms the manipulated coefficients to yield an image with enhanced contrast. Let $\bar{\mathbf{D}}$ denote the coefficient matrix after enhancement. In general, JPEG-domain enhancement can be formulated as a parametric mapping $f(\cdot, \lambda)$ from $\mathbf{D}$ to $\bar{\mathbf{D}}$:

$$\bar{\mathbf{D}} = f(\mathbf{D}, \lambda), \tag{2}$$

with λ the enhancement parameter. Different JPEG-domain enhancement methods can be regarded as different enhancement mappings.

For forensics analyzers, only the enhanced coefficient matrix $\bar{\mathbf{D}}$ is observable. The diversity of enhancement mapping f makes it challenging to directly model the characteristics of $\bar{\mathbf{D}}$. We recognize that regardless of the enhancement methods, $\bar{\mathbf{D}}$ is always enhanced from the quantized coefficient matrix $\mathbf{D}$, which exhibits periodicity in coefficient distribution [2]. If $\bar{\mathbf{D}}$ can be mapped back to $\mathbf{D}$ by a de-enhancement operation, the statistical modeling of JPEG-domain enhanced coefficients

can be transformed into the periodicity modeling of de-enhanced coefficients, which could be more easily solved. This is the basic idea behind the proposed likelihood function in the following.

B. De-Enhanced Coefficient Distribution

Denote the de-enhancement operator by $f^{-1}(\cdot, \lambda)$. Using the correct enhancement parameter $\lambda^\star$ to de-enhance $\bar{\mathbf{D}}$ can eliminate the influence of enhancement and yield

$$\mathbf{D}^\star = f^{-1}(\bar{\mathbf{D}}, \lambda^\star). \tag{3}$$

In the ideal situation, $\mathbf{D}^\star$ should be equal to $\mathbf{D}$, whose coefficients from any individual frequency should distribute exactly at $mq_{ij}, m \in \mathbb{Z}$, the multiples of the quantization step. However, in practical situations, $\bar{\mathbf{D}}$ contains some minor noise caused by pixel rounding, making the coefficients in $\mathbf{D}^\star$ deviate from mq_{ij} and distribute around it. Let $d_{ij}^\star$ denote the de-enhanced coefficient from the AC frequency (i, j) of $\mathbf{D}^\star$. The probability density of $d_{ij}^\star$ can be given by

$$p\left(d_{ij}^\star; q_{ij}\right) = \sum_{m\in\mathbb{Z}} P_L(mq_{ij}) G\left(d_{ij}^\star - mq_{ij}\right), \tag{4}$$

where $P_L(\cdot)$ is the quantized Laplacian probability mass function (PMF) that characterizes the probability of coefficient falling at mq_{ij} in the ideal noiseless situation, and $G(\cdot)$ is the truncated Gaussian probability density function (PDF) that characterizes the influence of rounding noise, which causes the coefficient deviate from mq_{ij} to some extent.

It is worth noting that the quantized Laplacian PMF is not the only option for characterizing quantized coefficients. Another PMF for quantized coefficients can be derived based on a doubly stochastic model, as proposed in [19]. However, Such a PMF has two extra distribution parameters, which additionally increases the complexity of the likelihood function for estimating the enhancement and compression parameters. In contrast, the quantized Laplacian PMF has only one distribution parameter and is thus preferable.

Specifically, $P_L(\cdot)$ has the form [13], [14], [18]:

$$P_L(x) = \int_{x-0.5q_{ij}}^{x+0.5q_{ij}} \frac{1}{2\rho_{ij}} \exp\left(-\frac{|u|}{\rho_{ij}}\right) du, \tag{5}$$

with ρ_{ij} the scale parameter of the Laplacian PDF being integrated, which can be estimated according to [14]. $G(\cdot)$ is the zero-mean truncated Gaussian PDF [13]:

$$G(x) = \begin{cases} \dfrac{1}{Z}\exp\left(-\dfrac{x^2}{2\sigma^2}\right) & \text{if } |x| \le B \\ 0 & \text{else} \end{cases}, \tag{6}$$

where σ^2 is the variance of rounding noise and takes the value of $1/12$ according to [13], [16], B is the bound of rounding noise and set to 4 according to [13], and Z is the scalar that normalizes the integration of $G(x)$ over the range $[-B, B]$ to 1, which can be calculated by

$$Z = \int_{-B}^{B} \frac{1}{\sqrt{2\pi}\,\sigma} \exp\left(-\frac{x^2}{2\sigma^2}\right) dx. \tag{7}$$

For $\sigma^2 = 1/12$, $B = 4$, we have $Z \approx 1 - 2.5979 \times 10^{-14} \approx 1$.

C. Likelihood Function Construction

With the distribution of de-enhanced coefficients given by Eq. (4), we can construct the likelihood function for estimating the enhancement parameter λ and compression parameter q_{ij}.

Given an enhanced coefficient matrix $\bar{\mathbf{D}}$, using different λ to de-enhance it will yield different de-enhanced coefficient matrix $\mathbf{D}(\lambda) = f^{-1}(\bar{\mathbf{D}}, \lambda)$. Let $d_{ij}^k(\lambda)$ denote the coefficients from the frequency (i, j) of $\mathbf{D}(\lambda)$, with k the index of 8×8 DCT blocks, $1 \le k \le K$. For each frequency (i, j), a likelihood function with respect to enhancement parameter λ and quantization step q_{ij} can be defined by

$$L_{ij}(\lambda, q_{ij}) \triangleq \frac{1}{K}\sum_{k=1}^{K} log\left(p\left(d_{ij}^k(\lambda); q_{ij}\right)\right). \tag{8}$$

The subscript ij in L_{ij} means that L_{ij} differs from frequency to frequency since the scale parameter ρ_{ij} in Eq. (5) depends on frequency. The sum of the likelihood values is normalized by the total number K of blocks to adapt preprocessing such as truncated/monotone block exclusion.

The true enhancement parameter should maximize L_{ij} for every frequency (i, j) and thus also maximize their sum over all frequencies of interest, which is given by

$$L(\lambda) \triangleq \sum_{(i,j)\in\mathcal{F}} \max_{1\le q_{ij}\le q_B} L_{ij}(\lambda, q_{ij}), \quad \lambda \in \mathcal{C}, \tag{9}$$

where $\mathcal{F}$ is the set of spatial frequencies (i, j) of interest, q_B is the upper bound of the quantization step, and $\mathcal{C}$ is the set of candidate enhancement parameters. The settings of $\mathcal{F}$, q_B and $\mathcal{C}$ are discussed in Section IV.

Therefore, the estimate of the enhancement parameter, denoted by $\hat{\lambda}$, can be obtained by

$$\hat{\lambda} = \arg\max_{\lambda\in\mathcal{C}} L(\lambda). \tag{10}$$

With the estimated $\hat{\lambda}$, the estimate of the quantization step for each (i, j), denoted by $\hat{q}_{ij}$, can be obtained by

$$\hat{q}_{ij} = \arg\max_{1\le q_{ij}\le q_B} L_{ij}(\hat{\lambda}, q_{ij}). \tag{11}$$

The enhancement parameter λ affects all frequencies, so it is estimated by the overall likelihood function $L(\lambda)$ that simultaneously considers multiple frequencies. In contrast, the quantization step q_{ij} only affects a single frequency (i, j), so it is estimated by the frequency-wise likelihood function $L_{ij}(\lambda, q_{ij})$.

At the end of this subsection, we briefly discuss the generalization of the proposed likelihood function. As presented, the above likelihood function is constructed based on the prerequisite that a given enhancement method has its de-enhancement operation. De-enhancement can be regarded as the reverse of enhancement. If an image operation has its corresponding reverse operation, the proposed likelihood function has the potential to forensically analyze images that have undergone JPEG compression followed by that operation. For example, if a JPEG image is gamma-corrected, the proposed likelihood function might be able to address the gamma-corrected image since gamma correction is reversible.

Many traditional image operations such as resampling and convolutional filtering are reversible. We believe the proposed likelihood function is also applicable to these operations with necessary modification.

IV. Proposed Forensic Method for JPEG-Domain Enhancement

In this section, we demonstrate the application of the proposed likelihood function to the forensic analysis of two classical methods of JPEG-domain enhancement, including:

- A non-recursive enhancement method proposed in [30]. This method weights the DCT coefficients by an enhancement factor for each frequency band independently in pursuit of real-time response and convenient use for people with vision impairment, who commonly need to adjust the contrast of an image interactively to meet their visual preference.
- A recursive enhancement method proposed in [31]. This method weights the DCT coefficients in a frequency band not only by the enhancement factor but also by the coefficients in previous frequency bands. Such a recursive manner helps to dynamically adjust the enhancement strength for each band at the cost of additional computation compared to [30].

The two classical methods of JPEG-domain enhancement have inspired many later proposed methods and usually serve as a benchmark for comparison. Their de-enhancement can be mathematically proven, which guarantees the applicability of the proposed likelihood function.

In the following, we first analyze the de-enhancement of the two enhancement methods and the difference between them, and then detail the proposed forensic method that can realize enhancement detection and parameter estimation in a unified framework.

A. De-Enhancement Analysis

1) De-Enhancement Analysis of the Method [30]: Similar to the notations used in Section III, let $f_{nr}(\cdot, \lambda_{nr})$ denote the non-recursive JPEG-domain enhancement with λ_{nr} the enhancement parameter. Enhancing a given coefficient d_{ij} with $f_{nr}(\cdot, \lambda_{nr})$ will yield

$$\bar{d}_{ij} = f_{nr}(d_{ij}, \lambda_{nr}) = \lambda_{nr}^{i+j} d_{ij}. \tag{12}$$

According to Eq. (12), the enhancement procedure can be briefly described as follows: divide an 8×8 DCT block into 15 different frequency bands, as shown in Fig. 1, and weight the coefficients in the t-th band by a factor of λ_{nr}^{t}. For example, the coefficients in the 0-th band are weighted by $\lambda_{nr}^{0} = 1$, while those in the 3-rd band are weighted by λ_{nr}^{3}.

Obviously, the de-enhancement operator $f_{nr}^{-1}(\cdot, \lambda_{nr})$ is the reverse function of $f_{nr}(\cdot, \lambda_{nr})$:

$$f_{nr}^{-1}(\bar{d}_{ij}, \lambda_{nr}) = d_{ij} = \left(\frac{1}{\lambda_{nr}}\right)^{i+j} \bar{d}_{ij} = f_{nr}\left(\bar{d}_{ij}, \frac{1}{\lambda_{nr}}\right). \tag{13}$$

Eq. (13) reveals a concise connection between the de-enhancement and enhancement of the non-recursive method: de-enhancement can be performed by enhancing the already enhanced coefficients with the reciprocal of the enhancement parameter.

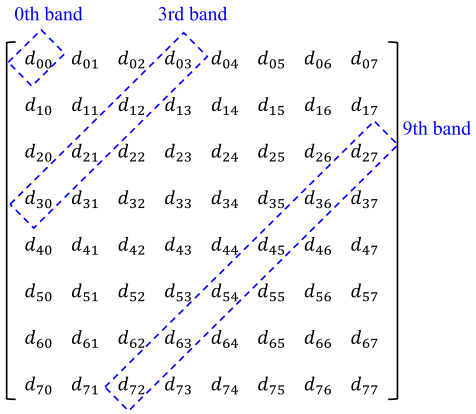

Fig. 1. Frequency band structure in the non-recursive [30] and the recursive [31] enhancement.

2) De-Enhancement Analysis of the Method [31]: The recursive enhancement method also manipulates the DCT coefficients in a band-wise manner, as shown in Fig. 1. Let $f_r(\cdot, \lambda_r)$ denote the recursive enhancement operator with λ_r the enhancement parameter. Enhancing a given coefficient d_{ij} with $f_r(\cdot, \lambda_r)$ will produce

$$\bar{d}_{ij} = f_r(d_{ij}, \lambda_r) = \begin{cases} d_{ij}, & i+j=0 \\ \lambda_r H_{i+j} d_{ij}, & i+j>0 \end{cases}, \tag{14}$$

where

$$H_\tau = \frac{\sum_{t=0}^{\tau-1} \bar{E}_t}{\sum_{t=0}^{\tau-1} E_t}. \tag{15}$$

E_t and $\bar{E}_t$ denote before and after enhancement, respectively, the averaged coefficient magnitude at band t:

$$E_t = \frac{1}{N_t} \sum_{i+j=t} |d_{ij}|, \tag{16}$$

where N_t is the number of frequencies at band t.

The term H_{i+j} in Eq. (14) differs not only from band to band but also from block to block. It is computed recursively, and thus, this method is termed "recursive" JPEG-domain enhancement. For more details please refer to [31].

Interestingly, the de-enhancement operator $f_r^{-1}(\cdot, \lambda_r)$ of the recursive enhancement has a similar form as that of the non-recursive enhancement:

$$f_r^{-1}(\bar{d}_{ij}, \lambda_r) = f_r\left(\bar{d}_{ij}, \frac{1}{\lambda_r}\right) \tag{17}$$

Eq. (17) can be proven by mathematical induction as follows:

Let $d'_{ij} = f_r\left(\bar{d}_{ij}, \frac{1}{\lambda_r}\right)$ and $d_{ij} = f_r^{-1}(\bar{d}_{ij}, \lambda_r)$ (the definition of de-enhancement), our goal is to prove $d'_{ij} = d_{ij}$ for all (i, j). The proof includes three steps:

1) For $i + j = 0$, $d'_{ij} = \bar{d}_{ij} = d_{ij}$ since the DC coefficient is kept unchanged according to Eq. (14).

2) For $i+j=1$,

$$\begin{aligned} d'_{ij} &= \frac{1}{\lambda_r}\bar{H}_{i+j}\bar{d}_{ij} \\ &= \frac{1}{\lambda_r}\bar{H}_{i+j}\left(\lambda_r H_{i+j} d_{ij}\right) \\ &= \bar{H}_1 H_1 d_{ij} = \frac{|d'_{00}|}{|\bar{d}_{00}|}\frac{|\bar{d}_{00}|}{|d_{00}|}d_{ij} = d_{ij}. \end{aligned} \tag{18}$$

In addition, we have

$$\begin{aligned} \bar{H}_2 H_2 &= \frac{\sum_{t=0}^{1}\bar{E}'_t}{\sum_{t=0}^{1}\bar{E}_t}\cdot\frac{\sum_{t=0}^{1}\bar{E}_t}{\sum_{t=0}^{1}E_t} = \frac{\sum_{t=0}^{1}\bar{E}'_t}{\sum_{t=0}^{1}E_t} \\ &= \frac{|d'_{00}|+|d'_{01}|+|d'_{10}|}{|d_{00}|+|d_{01}|+|d_{10}|} = 1. \end{aligned} \tag{19}$$

3) For $i+j=n\geq 1$, assume $d'_{ij}=d_{ij}$ holds. Accordingly, $\bar{H}_{n+1}H_{n+1}=1$ also holds. Then, for $i+j=n+1$, we have

$$\begin{aligned} d'_{ij} &= \frac{1}{\lambda_r}\bar{H}_{i+j}\bar{d}_{ij} \\ &= \frac{1}{\lambda_r}\bar{H}_{i+j}\left(\lambda_r H_{i+j} d_{ij}\right) \\ &= \bar{H}_{n+1}H_{n+1}d_{ij} = d_{ij}. \end{aligned} \tag{20}$$

By combining the above three steps, we finally arrive at $d'_{ij}=d_{ij}$ for all (i,j) and complete the proof of Eq. (17).

3) Analysis of Difference Between the Two Methods: The two enhancement methods mainly differ in the manner of coefficient weighting. That is, the non-recursive enhancement weights DCT coefficient d_{ij} with λ_{nr}^{i+j}, whereas the recursive enhancement weights it with $\lambda_r H_{i+j}$, as expressed in Eq. (12) and Eq. (14). When $\lambda_{nr}=\lambda_r=\lambda$, the following relationships always hold:

$$\begin{cases} \lambda^{i+j} \geq \lambda H_{i+j} \geq 1, & \lambda > 1 \\ \lambda^{i+j} \leq \lambda H_{i+j} \leq 1, & \lambda < 1 \end{cases}, \tag{21}$$

which means that the non-recursive enhancement changes the coefficient more heavily than the recursive enhancement under the same enhancement parameter.

Eq. (21) can be proven by mathematical induction as follows:

According to the definition of H_{i+j} in Eq. (15), $\lambda>1$ leads to $H_{i+j}\geq 1$ and then $\lambda H_{i+j}\geq 1$. Similarly, $\lambda<1$ leads to $H_{i+j}\leq 1$ and then $\lambda H_{i+j}\leq 1$. Hence, the remaining is to prove the relationship between λ^{i+j} and λH_{i+j}, which includes three steps:

1) For $i+j=1$, we have $\lambda H_1 = \lambda\frac{|\bar{d}_{00}|}{|d_{00}|}=\lambda^1$, so Eq. (21) holds. In addition, we have $\bar{E}_0 = E_0$ and $\bar{E}_1 = \lambda H_1\ E_1 = \lambda E_1$.
2) For $i+j=2$, we have

$$\begin{aligned} \lambda H_2 &= \lambda\frac{\sum_{t=0}^{1}\bar{E}_t}{\sum_{t=0}^{1}E_t} = \lambda\frac{\bar{E}_0+\bar{E}_1}{E_0+E_1} \\ &= \lambda\frac{E_0+\lambda E_1+\lambda E_0-\lambda E_0}{E_0+E_1} \\ &= \lambda\left[\lambda+(1-\lambda)\frac{E_0}{E_0+E_1}\right]. \end{aligned} \tag{22}$$

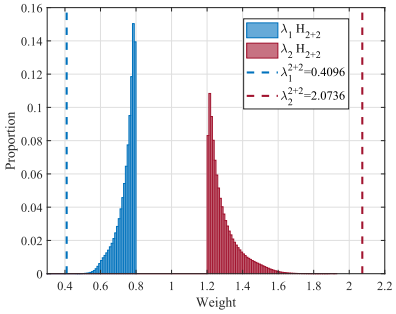

Fig. 2. Distribution of weights for the non-recursive [30] and the recursive [31] enhancement.

Both E_0 and E_1 are non-negative, so $0\leq\frac{E_0}{E_0+E_1}\leq 1$. It can be discussed in two cases:

- If $\lambda>1$, then $(1-\lambda)<0$, so $\lambda\leq\lambda H_2\leq\lambda^2$.
- If $\lambda<1$, then $(1-\lambda)>0$, so $\lambda^2\leq\lambda H_2\leq\lambda$.

Combining the two cases, Eq. (21) holds for $i+j=2$. In addition, we further have

$$\begin{cases} \bar{E}_2 = \lambda H_2 E_2 \leq \lambda^2 E_2, & \lambda > 1 \\ \bar{E}_2 = \lambda H_2 E_2 \geq \lambda^2 E_2, & \lambda < 1 \end{cases}. \tag{23}$$

3) For $i+j=n\geq 2$, assume Eq. (21) holds. We accordingly have

$$\begin{cases} \bar{E}_n = \lambda H_n E_n \leq \lambda^n E_n, & \lambda > 1 \\ \bar{E}_n = \lambda H_n E_N \geq \lambda^n E_n, & \lambda < 1 \end{cases}. \tag{24}$$

Then, for $i+j=n+1$, we can rewrite λH_{n+1} as

$$\begin{aligned} \lambda H_{n+1} &= \lambda\frac{\sum_{t=0}^{n}\bar{E}_t}{\sum_{t=0}^{n}E_t} = \lambda\frac{\sum_{t=0}^{n-1}\bar{E}_t+\bar{E}_n}{\sum_{t=0}^{n-1}E_t+E_n} \\ &= \lambda\frac{\sum_{t=0}^{n-1}\bar{E}_t+\bar{E}_n+\lambda^n\sum_{t=0}^{n-1}E_t-\lambda^n\sum_{t=0}^{n-1}E_t}{\sum_{t=0}^{n-1}E_t+E_n} \\ &= \lambda\left[\frac{\bar{E}_n+\lambda^n\sum_{t=0}^{n-1}E_t}{\sum_{t=0}^{n-1}E_t+E_n}+\frac{\sum_{t=0}^{n-1}(\bar{E}_t-\lambda^n E_t)}{\sum_{t=0}^{n-1}E_t+E_n}\right] \\ &\triangleq \lambda(A+B). \end{aligned} \tag{25}$$

Similarly, it can be discussed in two cases:

- If $\lambda>1$, then $A\leq\lambda^n$ and $B\leq 0$ according to Eq. (24), so $\lambda H_{n+1}=\lambda(A+B)\leq\lambda(\lambda^n+0)=\lambda^{n+1}$.
- If $\lambda<1$, then $A\geq\lambda^n$ and $B\geq 0$ according to Eq. (24), so $\lambda H_{n+1}=\lambda(A+B)\geq\lambda(\lambda^n+0)=\lambda^{n+1}$.

Therefore, Eq. (21) holds for $i+j=n+1$ if it holds for $i+j=n$.

By combining all three steps, we finally complete the proof of Eq. (21) via mathematical induction.

To illustrate the above analysis, Fig. 2 gives the distribution of λH_{i+j} and the value of λ^{i+j} for the frequency $(i,j)=(2,2)$. Each distribution contains 6690 samples, which are generated by JPEG compressing the 1338 UCID images with QF $\in\{50,60,70,80,90\}$ and then enhancing the resulting JPEG images with $\lambda_1=0.8$ and $\lambda_2=1.2$. For $\lambda_1=0.8<1$, the recursive enhancement weights the coefficients with $\lambda_1\ H_{2+2}$ (the blue bins), while the non-recursive

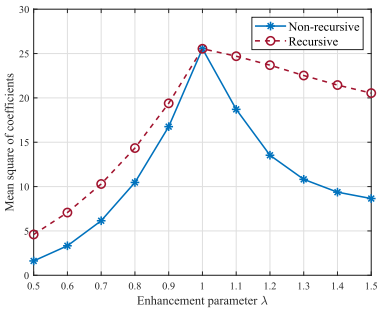

Fig. 3. Mean squares of coefficients for the non-recursive [30] and the recursive [31] enhancement.

enhancement weights the coefficients with a fixed value of $\lambda_1^{2+2} = 0.4096$ (the blue dashed line). Obviously, $\lambda_1^{2+2} \leq \lambda_1\ H_{2+2} < 1$, which implies that the recursive enhancement weights the coefficients more mildly and thus causes less change to the coefficients than the non-recursive enhancement. Similarly, for $\lambda_2 = 1.2 > 1$, we can observe $\lambda_1^{2+2} \geq \lambda_1\ H_{2+2} > 1$, also indicating that the recursive enhancement weights coefficients more mildly.

Fig. 3 further shows the mean squares of coefficients varying with different enhancement parameters λ for the two enhancement methods, which are computed from 6690 images by excluding monotone and saturated blocks. Generally, a large mean square implies that a high proportion of large coefficients are available for forensic analysis. Two observations can be obtained. First, the mean square decreases when λ increases or decreases away from 1, and the decreasing is faster when $\lambda < 1$ than when $\lambda > 1$. This can be explained as follows. When $\lambda > 1$, a larger λ leads to more saturated blocks but meanwhile larger coefficients, which can compensate each other and slow down the decreasing of the mean square. In contrast, when $\lambda < 1$, a smaller λ leads to not only more monotone blocks but also smaller coefficients, which together decrease the mean square and make the decreasing faster. Second, the mean square of coefficients for the recursive enhancement decreases slower than the non-recursive one, further validating the above analysis that the recursive enhancement enhances an image more mildly. In summary, it is expected that the forensic analysis of the non-recursive enhancement will be more difficult since fewer/smaller coefficients are available, especially in the cases of $\lambda < 1$.

B. Proposed Forensic Method

With the de-enhancement operators derived above, the proposed likelihood function is ready for enhancement detection and parameter estimation. For both the non-recursive and the recursive JPEG-domain enhancement, the following relationship holds:

$$f(d_{ij}, 1) = d_{ij}. \tag{26}$$

Eq. (26) indicates that an original coefficient d_{ij} enhanced with enhancement parameter 1 is equal to itself. In other words, an original (non-enhanced) image can be regarded as an enhanced image with enhancement parameter 1. It is

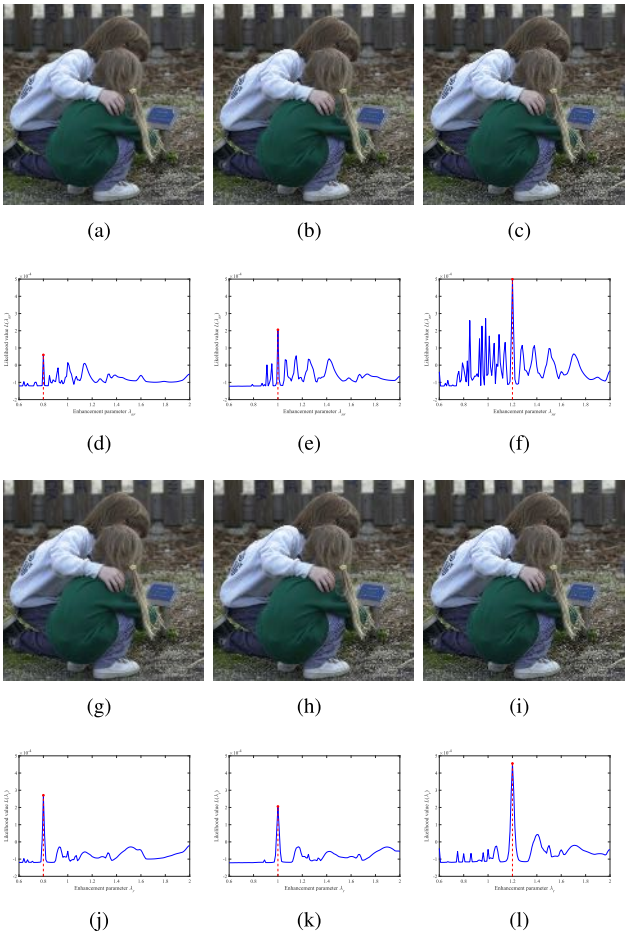

Fig. 4. Curves of the overall likelihood function for different degrees of enhancement. (a) Non-recursive enhancement with $\lambda_{nr} = 0.8$; (b) original image ($\lambda_{nr} = 1.0$); (c) non-recursive enhancement with $\lambda_{nr} = 1.2$; (d)–(f) curves of $L(\lambda_{nr})$ corresponding to (a)–(c), respectively. (g) Recursive enhancement with $\lambda_r = 0.8$; (h) original image ($\lambda_r = 1.0$); (i) recursive enhancement with $\lambda_r = 1.2$; (j)–(l) curves of $L(\lambda_r)$ corresponding to (g)–(i), respectively. The PSNR between (a) and (b) is $\text{PSNR}_{a,b} = 36.43$ dB. Similarly, $\text{PSNR}_{c,b} = 32.90$ dB, $\text{PSNR}_{g,h} = 39.62$ dB, $\text{PSNR}_{i,h} = 39.11$ dB.

interesting to mention that many traditional image manipulations also have similar relationships between non-manipulated images and manipulated images. For instance, a non-resized image can be regarded as a resized image with a resizing ratio of 1, or a non-gamma-corrected image can be viewed as a gamma-corrected image with a gamma value of 1. Based on the relationship revealed by Eq. (26), the overall likelihood function $L(\lambda)$ proposed in Eq. (9) has the following properties (the subscripts of λ_r and λ_{nr} are omitted for clarity if unnecessary):

- For an original image, $L(\lambda)$ is expected to reach its maximum at 1.
- For an enhanced image, $L(\lambda)$ should be maximized at the true value of the enhancement parameter.

To illustrate these properties, the curves of the overall likelihood function for different degrees of enhancement are shown in Fig. 4. Only the luminance component of the color image is enhanced while keeping the chrominance components unchanged. For the non-recursive enhancement [30],

the images enhanced with $\lambda_{nr} = 0.8$ and 1.2 are shown in (a) and (c), respectively, with the original image shown in (b). The likelihood curves corresponding to images (a)–(c) are shown in (d)–(f), respectively. The ranges of the vertical axes (likelihood value) in (d)–(f) are kept consistent for convenience of comparison. Note that enhancing with $\lambda_{nr} < 1$ will decrease the sharpness of the edges and textures (such as the "hair" and "rubble" regions of the sample image) and result in a relatively smooth image, as shown in (a), whereas enhancing with $\lambda_{nr} > 1$ will sharpen these details, as shown in (c). For the enhanced images (a) and (c), their corresponding likelihood curves reach the maximum at 0.8 and 1.2, respectively, which are exactly equal to the truly used enhancement parameter; for the original image (b), the maximum of its likelihood curve occurs at 1. Similar observations can be made for the recursive enhancement [31], as shown in (g)–(l). The peak signal to noise ratios (PSNRs) between the enhanced images and the original image are also computed: $\text{PSNR}_{a,b} = 36.43$ dB, $\text{PSNR}_{c,b} = 32.90$ dB, $\text{PSNR}_{g,h} = 39.62$ dB, and $\text{PSNR}_{i,h} = 39.11$ dB. Note that (a) and (g) are enhanced with the same value of enhancement parameter ($\lambda_{nr} = \lambda_r = 0.8$), but $\text{PSNR}_{a,b} = 36.43$ dB $< \text{PSNR}_{g,h} = 39.62$ dB, which means that the "distortion" caused by the recursive enhancement is slighter than that caused by the non-recursive enhancement. Similarly, $\text{PSNR}_{c,b} = 32.90$ dB $< \text{PSNR}_{i,h} = 39.11$ dB for $\lambda_{nr} = \lambda_r = 1.2$. These results imply that the recursive enhancement is milder than the non-recursive enhancement, as analyzed in the previous subsection.

Based on these properties, a simple yet effective thresholding detector is proposed to detect the presence of enhancement. First, a scalar feature s can be defined as:

$$s \triangleq \max_{\lambda \neq 1} L(\lambda) - L(1). \tag{27}$$

Then, a given image I is detected to be an original image if $s < 0$ since $L(1)$ is the maximum of $L(\lambda)$; otherwise, it is detected to be an enhanced image.

Since enhancement detection can be regarded as a classification task, another possible solution is to train a binary classifier that directly takes the likelihood values $L(\lambda)$ as features. Such a learning-based approach is promising because it can make better use of the discriminability of the likelihood values but has to perform classifier training. In contrast, the above-proposed thresholding detector is free from training yet highly effective in enhancement detection as reported in Section V-B. It is also more intuitive for demonstrating the property of $L(\lambda)$ and is thus preferred.

Once I is detected to be an enhanced image, its enhancement parameter can be estimated according to Eq. (10), and its compression parameter (namely, quantization steps) can be estimated according to Eq. (11).

In summary, the proposed forensic method for enhancement detection and parameter estimation is illustrated in Fig. 5 and described as follows.

1) Given an image I, divide I into non-overlapping 8×8 blocks and exclude saturated blocks and monotone blocks. A saturated block is a block containing any pixel with a value of 0 or 255, while a monotone block is a block containing pixels with the same value. The former is contaminated by truncation noise, and the latter provides little discriminative information, both of which are unsuitable for likelihood computation and thus excluded.
2) Compute the scalar feature s for enhancement detection according to Eq. (27).
3) I is detected to be an original (non-enhanced) image if $s < 0$; otherwise, it is detected to be an enhanced image.
4) Estimate the enhancement parameter λ according to Eq. (10) if I is detected to be enhanced.
5) Substitute the estimated enhancement parameter $\hat{\lambda}$ into Eq. (11) to obtain the estimate $\hat{q}_{ij}$ of quantization steps.

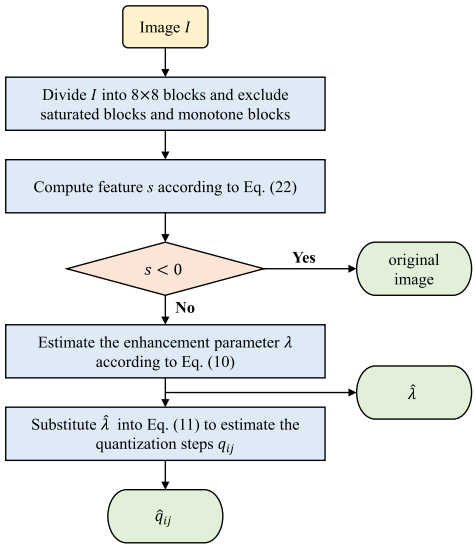

Fig. 5. Flowchart of the proposed forensic method for enhancement detection and parameter estimation.

It is worth noting that the proposed method works in a manner similar to hypothesis testing. That is, it first assumes that the image to be detected has been enhanced and accepts the assumption if $s > 0$. The enhancement parameter and compression parameter can be further estimated if the assumption is accepted.

When implementing the above-proposed method, the settings of $\mathcal{F}$, q_B and $\mathcal{C}$ in Eq. (9) are crucial to reproducing the reported results in Section V. Empirically, we set $\mathcal{F} = \{(0, 1), (0, 2), (0, 3), (1, 0), (1, 1), (1, 2), (2, 0), (2, 1), (3, 0)\}$, which includes the first nine low frequencies in zigzag order. Excessively high frequencies are not considered because they usually do not have sufficient non-zero coefficients to support a reliable computation of likelihood. We set $q_B = 25$ since 25 is large enough to cover the range of quantization step corresponding to frequencies in $\mathcal{F}$ when QF ≤ 50, the commonly used range of quality factors for JPEG compression. The setting of $\mathcal{C}$ is slightly different for the two JPEG-domain enhancement methods. For the non-recursive enhancement [30], $\mathcal{C}$ is set from 0.60 to 2.00 with a step of 0.05 to cover the commonly used range of enhancement parameter, namely, $\mathcal{C} = \{0.60, 0.65, \cdots, 2.00\}$; for the recursive enhancement [31], $\mathcal{C} = \{0.60, 0.65, \cdots, 3.30\}$. As discussed in Section IV-A3, in contrast to the non-recursive enhancement, the recursive

enhancement weights DCT coefficients more mildly, and thus can support a wider range of enhancement parameters.

V. Experimental Evaluation

This section first presents the experimental settings and then reports the performance of the proposed method in three aspects: enhancement detection, enhancement parameter estimation, and compression parameter estimation.

A. Experimental Settings

1) Sample Generation: The UCID [41] image set, consisting of 1338 images with a size of 384×512 pixels, is used to generate sample images for evaluation. The UCID images are JPEG compressed with QF $\in \{50, 60, 70, 80, 90\}$. These resulting JPEG images are decompressed to produce a total of $1338 * 5 = 6690$ original (non-enhanced) images. Enhanced images are also generated based on these resulting JPEG images. For the non-recursive enhancement, these JPEG images are enhanced with $\lambda_{nr} \in \{0.7 : 0.1 : 0.9, 1.1 : 0.1 : 1.5\}$ (namely, increasing with a step of 0.1); for the recursive enhancement, they are enhanced with $\lambda_r \in \{0.7 : 0.1 : 0.9, 1.1 : 0.1 : 1.5, 1.6 : 0.2 : 3.0\}$. As a result, $1338*5*8 = 53520$ and $1338*5*16 = 107040$ enhanced image are generated for the non-recursive and the recursive enhancement, respectively. Note that both the original and enhanced images are saved in the lossless image format. Our forensic goal is to detect the enhanced images and estimate both the enhancement and compression parameters.

2) Performance Measurement: Detection accuracy, defined by (true positive rate + true negative rate)$/2 * 100\%$, is used to quantify the performance of enhancement detection, where the true positive (negative) rate is the proportion of correctly detected enhanced (original) images to the total enhanced (original) images.

Estimation accuracy is used to measure the performance of parameter estimation, which is defined as the proportion of correct estimates to the total estimates. Since the enhancement parameter is floating-point-valued and the compression parameter (quantization step) is integer-valued, their criteria of "correctness" are slightly different. For enhancement parameter estimation, an estimate is considered to be correct if the absolute difference between the estimate and the true value is less than a tolerance (0.025 is set in the experiments). For compression parameter estimation, an estimate is considered to be correct only if it is exactly equal to the true value. The estimation accuracy of the quantization step is evaluated over the first nine spatial frequencies in zigzag order.

3) Compared Methods: Although there is no previous forensic method directly proposed for JPEG-domain enhancement in the current literature, some methods have the potentiality to partially address the forensics of JPEG-domain enhancement if properly used, as stated in the following.

For comparison of enhancement detection, three feature sets are implemented, which are based on edge perpendicular binary coding (EPBC) [42], reduced spatial rich model (RSRM) [43] and threshold local binary pattern (TLBP) [44], respectively. These feature sets are good at capturing the statistical abnormality induced by image operations and are expected to also be effective for characterizing the mixed artifacts caused by JPEG-domain enhancement. Half of the image samples generated above are used to train a binary ensemble classifier [45] for each feature set, and the other half are used for testing. When compared with these three methods, the proposed method are also evaluated on the same test images for a valid comparison.

For comparison of enhancement parameter estimation, inspired by [43], multi-class ensemble classification is implemented for the three feature sets with the one-versus-rest strategy. By regarding each enhancement parameter as an individual class, for each of the three feature sets, a nine-class classifier is trained for the non-recursive enhancement to estimate λ_{nr} from $\{0.7 : 0.1 : 1.5\}$, and a seventeen-class classifier is trained for the recursive enhancement to estimate λ_r from $\{0.7 : 0.1 : 1.5, 1.6 : 0.2 : 3.0\}$. Note that such a comparison is somewhat unfair to our proposed method since our method performs the estimation in a wider range and a finer grain. All of the multi-class classifiers are trained on half of the image samples and tested on the other half.

For comparison of compression parameter estimation, five existing methods are implemented, including Ye *et al.*'s [15], Luo *et al.*'s [16], Lin *et al.*'s [17], Thai *et al.*'s [19], and Yang *et al.*'s [20]. Since these five methods and the proposed method are free from training, their performance is tested on all of the image samples. Note that the compression parameter (namely, quantization steps) is estimated frequency by frequency. The above three feature sets are unsuitable for compression parameter estimation since they are extracted from the whole image rather than from an individual frequency.

B. Enhancement Detection

Fig. 6 and 7 show the distributions of the scalar feature s for detecting the non-recursive and the recursive enhancement, respectively. The s distributions of original images and enhanced images are plotted in red and blue, respectively. Each distribution is normalized to sum to 1 for convenient comparison.

Two observations are obtained. First, the s of either original or enhanced images show relatively large intra-class variations. As stated above, original images are generated using different compression parameters and enhanced images are generated under various degrees of compression and enhancement. The diversity of image samples leads to a relatively large variation in s. Second, the s of original images can be clearly distinguished from those of enhanced images. Table II further lists the true positive rates (TPRs), true negative rates (TNRs) and detection accuracies (ACCs) under different QFs for the non-recursive enhancement (NRE) and the recursive enhancement (RE), respectively. In all test cases, the detection accuracies of the proposed method are up to 99% or more, indicating the effectiveness of s in enhancement detection.

Table III reports the detection accuracies achieved by the compared feature sets and the proposed scale feature. The RSRM and TLBP feature sets can achieve the accuracies of 90% or higher for all test cases, indicating that these

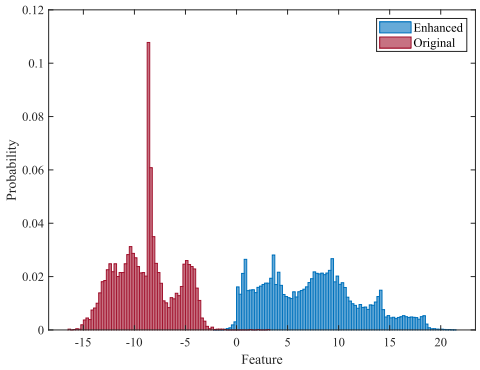

Fig. 6. Distribution of the proposed scalar feature s for detecting the non-recursive enhancement.

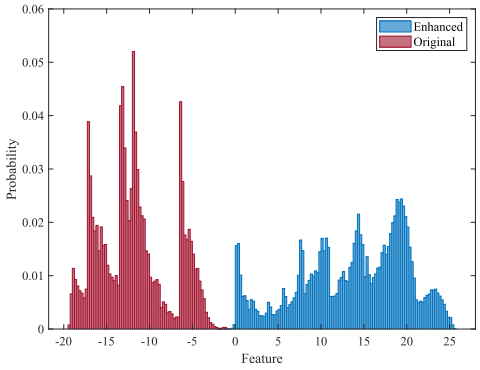

Fig. 7. Distribution of the proposed scalar feature s for detecting the recursive enhancement.

TABLE II

PERFORMANCE (%) OF THE PROPOSED FEATURE s IN DETECTING THE NON-RECURSIVE ENHANCEMENT (NRE) [30] AND THE RECURSIVE ENHANCEMENT (RE) [31]

QF		50	60	70	80	90
NRE	TPR	100	99.94	99.90	98.05	98.85
	TNR	100	100	100	100	99.78
	ACC	100	99.97	99.95	99.03	99.31
RE	TPR	100	100	99.98	99.93	99.86
	TNR	100	100	100	100	100
	ACC	100	100	99.99	99.96	99.93

high-dimensional feature sets have good discriminability for enhancement detection. In contrast, the proposed feature is only one-dimensional but significantly outperforms the compared feature sets, validating its high efficiency in capturing the artifacts caused by JPEG-domain enhancement.

C. Enhancement Parameter Estimation

Table IV and Table V show the estimation accuracies of the enhancement parameter for the non-recursive and the recursive enhancement, respectively. More cases are tested for the recursive enhancement since it enhances images more mildly than the non-recursive enhancement, and thus supports a wider range of enhancement parameters. Recall the discussion in Section IV-B that an original image is equivalent to an enhanced image with an enhancement parameter of 1. Therefore, the estimation accuracies of enhancement parameter on original images are also given in the rows "1.0" of the two tables. The estimation accuracies are beyond 95% in most test cases, indicating the proposed method can be applicable to a variety of combinations of enhancement parameters and compression parameters.

TABLE III

COMPARISON OF ACCURACIES (%) IN DETECTING THE NON-RECURSIVE ENHANCEMENT (NRE) [30] AND THE RECURSIVE ENHANCEMENT (RE) [31]

QF		50	60	70	80	90
NRE	EPBC [42]	86.40	88.02	89.12	89.19	87.66
	RSRM [43]	94.94	94.58	95.25	94.62	93.81
	TLBP [44]	96.57	96.28	96.45	95.20	96.12
	Proposed	**100**	**99.95**	**99.91**	**98.87**	**99.06**
RE	EPBC [42]	81.46	81.54	82.41	82.20	81.93
	RSRM [43]	95.73	94.31	95.42	93.09	91.93
	TLBP [44]	94.64	93.07	92.66	92.69	90.45
	Proposed	**100**	**100**	**99.98**	**99.92**	**99.90**

TABLE IV

ACCURACIES (%) OF THE PROPOSED METHOD IN ESTIMATING THE QUANTIZATION STEPS q_{ij} IN THE PRESENCE OF THE NON-RECURSIVE ENHANCEMENT [30]

λ_{nr} \ QF	50	60	70	80	90
0.7	51.20	66.97	90.58	59.42	0.00
0.8	99.85	99.63	99.48	98.21	43.35
0.9	100	100	100	99.85	98.80
1.0	100	100	100	100	99.78
1.1	99.93	99.93	99.85	99.85	99.10
1.2	99.55	99.55	98.73	99.18	98.73
1.3	97.61	98.65	98.73	98.36	97.98
1.4	95.81	90.66	95.96	87.82	94.25
1.5	95.59	84.23	81.02	85.65	77.88

TABLE V

ACCURACIES (%) OF THE PROPOSED METHOD IN ESTIMATING THE QUANTIZATION STEPS q_{ij} IN THE PRESENCE OF THE RECURSIVE ENHANCEMENT [31]

λ_r \ QF	50	60	70	80	90
0.7	100	100	100	99.93	87.59
0.8	100	100	100	100	99.70
0.9	100	100	100	100	100
1.0	100	100	100	100	100
1.1	100	100	100	100	100
1.2	99.93	100	100	100	100
1.3	99.55	99.85	100	100	99.93
1.4	99.85	99.93	99.85	99.93	99.78
1.5	99.48	99.78	99.63	99.85	99.70
1.6	99.33	99.55	99.55	99.48	99.55
1.8	99.18	99.63	99.10	99.18	99.03
2.0	98.58	99.10	98.80	98.58	98.13
2.2	97.76	97.61	97.61	98.06	96.94
2.4	96.56	97.68	97.16	97.09	95.74
2.6	95.14	96.41	95.96	96.64	94.02
2.8	93.95	93.57	93.95	95.74	91.55
3.0	92.53	94.02	90.43	93.50	89.09

TABLE VI

COMPARISON OF ACCURACY (%) IN ESTIMATING THE ENHANCEMENT PARAMETER λ_{nr} FOR THE NON-RECURSIVE ENHANCEMENT [30]

λ_{nr} \ Method	EPBC [42]	RSRM [43]	TLBP [44]	Proposed
0.7	55.67	78.48	**87.92**	55.99
0.8	52.97	86.55	**91.60**	87.80
0.9	58.09	89.78	95.22	**99.73**
1.0	54.26	85.74	94.92	**99.94**
1.1	39.49	85.08	87.92	**99.46**
1.2	42.87	90.08	89.72	**98.42**
1.3	39.01	85.41	88.73	**96.95**
1.4	44.69	83.50	88.91	**89.92**
1.5	47.77	83.86	**91.42**	81.10

TABLE VII

COMPARISON OF ACCURACIES (%) IN ESTIMATING THE ENHANCEMENT PARAMETER λ_r FOR THE RECURSIVE ENHANCEMENT [31]

λ_r \ Method	EPBC [42]	RSRM [43]	TLBP [44]	Proposed
0.7	23.38	64.51	73.99	**96.80**
0.8	40.90	70.49	73.00	**99.94**
0.9	42.15	77.46	74.53	**100**
1.0	33.93	71.78	78.48	**100**
1.1	26.85	68.28	67.95	**100**
1.2	25.77	70.43	65.83	**99.97**
1.3	28.64	53.81	60.39	**99.73**
1.4	24.99	73.27	55.81	**99.73**
1.5	19.10	58.77	51.78	**99.37**
1.6	18.03	71.87	66.01	**98.98**
1.8	15.75	73.03	64.45	**98.45**
2.0	19.22	73.81	64.48	**97.37**
2.2	25.74	67.32	67.32	**95.81**
2.4	17.76	68.49	67.62	**94.56**
2.6	14.83	74.50	66.73	**93.15**
2.8	22.30	66.97	61.70	**90.97**
3.0	11.06	70.97	61.78	**88.52**

TABLE VIII

ACCURACIES (%) OF THE PROPOSED METHOD IN ESTIMATING THE QUANTIZATION STEPS q_{ij} IN THE PRESENCE OF THE NON-RECURSIVE ENHANCEMENT [30]

λ_{nr} \ QF	50	60	70	80	90
0.7	27.64	33.38	47.04	17.16	1.49
0.8	88.52	94.95	92.04	85.01	15.45
0.9	98.75	99.67	99.58	96.63	98.97
1.0	99.86	99.91	99.34	99.19	99.78
1.1	99.50	99.90	99.75	99.42	99.06
1.2	95.53	99.53	98.69	99.08	98.56
1.3	96.40	98.57	98.67	98.22	97.79
1.4	95.70	90.64	95.93	87.60	94.25
1.5	95.54	84.21	80.97	85.65	77.96

TABLE IX

ACCURACIES (%) OF THE PROPOSED METHOD IN ESTIMATING THE QUANTIZATION STEPS q_{ij} IN THE PRESENCE OF THE RECURSIVE ENHANCEMENT [31]

λ_r \ QF	50	60	70	80	90
0.7	94.65	98.41	96.94	94.03	71.83
0.8	98.19	99.79	98.41	96.27	99.49
0.9	99.60	99.89	99.93	98.40	99.99
1.0	99.85	99.91	99.34	99.19	99.99
1.1	99.69	99.97	99.97	99.66	99.95
1.2	96.70	99.93	100	99.94	99.95
1.3	98.82	99.74	100	99.92	99.97
1.4	99.78	99.88	99.84	99.73	99.83
1.5	99.28	99.75	99.49	99.84	99.68
1.6	99.14	99.51	99.57	99.45	99.45
1.8	99.13	99.51	99.12	99.14	99.03
2.0	98.56	99.09	98.79	98.58	98.13
2.2	97.64	97.66	97.60	98.05	96.93
2.4	96.53	97.68	97.13	96.99	95.67
2.6	95.08	96.39	95.89	96.55	94.02
2.8	93.86	93.53	93.85	95.67	91.62
3.0	92.47	93.99	90.43	93.43	89.21

Two phenomena can be observed in Tables IV and V. First, the estimation accuracies for the recursive enhancement are higher than those for the non-recursive enhancement. Second, for a fixed QF, the accuracy mostly achieves its maximum at row "1.0" and then gradually decreases with either a decrease or increase in the enhancement parameter. As analyzed in Section IV-A3, the recursive enhancement weights coefficients more mildly so that the coefficients available for estimation are more sufficient, which helps to achieve better accuracies. Fig. 3 gives a more intuitive interpretation. The curve of the coefficient mean square for the non-recursive enhancement is always below that for the recursive enhancement, implying that fewer/smaller coefficients are available for the parameter estimation of the non-recursive enhancement. Moreover, both curves decrease more rapidly when $\lambda < 1$ than when $\lambda > 1$. When λ reaches 0.7, the mean square for the non-recursive enhancement has already decreased to a very low level, as shown in Fig. 3. So the corresponding estimation accuracies in Table IV are far from satisfactory. Please refer to Section IV-A3 for a more detailed discussion.

Tables VI and VII report the accuracies of the three feature sets and the proposed method in estimating λ_{nr} and λ_r, respectively. Interestingly, the EPBC, RSRM and TLBP feature sets achieve lower accuracies in estimating λ_r than estimating λ_{nr}. The main reason is that the ensemble classifier for estimating λ_r includes 17 classes, whereas that for estimating λ_{nr} only includes 9 classes. Distinguishing between more classes is generally more difficult and leads to lower accuracy. In comparison with these three methods, the proposed method shows its superiority in most of the test cases.

D. Compression Parameter Estimation

Tables VIII and V report the estimation accuracies of the quantization step q_{ij} for the two enhancement methods. In most test cases, the proposed method can achieve an estimation accuracy of 90% or more, showing its wide applicability to various test settings.

There are two observations. First, for a fixed QF, the estimation accuracy usually reaches its maximum when the tested enhancement parameter is 1 or close to 1, and gradually decreases with either a decrease or increase in the enhancement parameter. This behavior, similar to that discussed in

TABLE X

COMPARISON OF ACCURACIES (%) IN ESTIMATING THE QUANTIZATION STEPS q_{ij} IN THE PRESENCE OF THE NON-RECURSIVE ENHANCEMENT [30]

Method / λ_{nr}	Ye *et al.* [15]	Luo *et al.* [16]	Lin *et al.* [17]	Thai *et al.* [19]	Yang *et al.* [20]	Proposed
0.7	1.05	2.53	0.00	0.01	0.01	**25.34**
0.8	3.29	5.14	0.00	0.01	0.01	**75.19**
0.9	18.17	9.86	6.11	0.03	0.03	**98.72**
1.0	96.12	98.14	98.94	99.77	**99.79**	99.62
1.1	12.30	8.88	6.00	0.03	0.03	**99.53**
1.2	8.51	2.30	0.91	0.01	0.00	**98.28**
1.3	8.06	0.11	0.00	0.00	0.01	**97.93**
1.4	4.15	0.12	0.00	0.57	0.52	**92.82**
1.5	2.13	0.16	0.01	0.01	0.03	**84.87**

TABLE XI

COMPARISON OF ACCURACIES (%) IN ESTIMATING THE QUANTIZATION STEPS q_{ij} IN THE PRESENCE OF THE RECURSIVE ENHANCEMENT [31]

Method / λ_r	Ye *et al.* [15]	Luo *et al.* [16]	Lin *et al.* [17]	Thai *et al.* [19]	Yang *et al.* [20]	Proposed
0.7	1.10	0.22	0.00	0.01	0.01	**91.17**
0.8	5.82	4.28	0.15	0.02	0.02	**98.43**
0.9	18.35	22.83	16.61	0.05	0.06	**99.56**
1.0	96.11	98.14	98.94	99.77	**99.79**	99.66
1.1	19.44	22.44	26.85	0.04	0.04	**99.85**
1.2	15.10	4.71	2.38	0.00	0.00	**99.30**
1.3	8.10	0.01	0.00	0.00	0.00	**99.69**
1.4	12.57	0.01	0.00	0.00	0.00	**99.81**
1.5	10.61	0.01	0.00	0.00	0.00	**99.61**
1.6	10.23	0.01	0.00	0.00	0.01	**99.42**
1.8	6.44	0.02	0.00	0.00	0.01	**99.19**
2.0	4.52	0.03	0.02	0.95	0.95	**98.63**
2.2	4.55	0.04	0.01	0.00	0.00	**97.58**
2.4	2.90	0.04	0.16	0.00	0.00	**96.80**
2.6	2.79	0.04	0.00	0.00	0.00	**95.59**
2.8	1.98	0.04	0.00	0.06	0.01	**93.71**
3.0	1.53	0.05	0.01	0.82	3.25	**91.91**

Section V-C, is mainly caused by the reduction of coefficients available for estimation.

Second, comparing the same test cases in Table IV with Table VIII (or Table V with Table IX), we can observe that in most cases the estimation accuracy of the quantization step (Table VIII) is slightly lower than that of the enhancement parameter (Table IV). This is because the estimation of the quantization step is affected by the estimation error of the enhancement parameter, making it usually have lower accuracy. Surprisingly, several test cases reveal that the estimation accuracy of the quantization step can also be higher than that of the enhancement parameter. Taking the case of $(\lambda_{nr}, \text{QF}) = (0.9, 90)$ in Table VIII as an example, the estimation accuracy of the quantization step is 98.97%, which is higher than 98.80%, the estimation accuracy of the enhancement parameter reported in Table IV. After analyzing these cases, we found out the cause. As stated in Subsection V-A2, an estimate of the enhancement parameter is considered to be correct only if the estimate deviates from the true value less than a tolerance of 0.025. When an estimate of the enhancement parameter is slightly beyond the tolerance, it is considered as an incorrect estimate, but such slight error sometimes would not mislead the estimation of the quantization steps, hence resulting in the above surprising but interpretable phenomenon.

Accuracy comparisons of quantization step estimation are listed in Tables X and XI. For original (non-enhanced) images, the compared methods can estimate the quantization steps precisely, and Yang *et al.*'s method (improved upon Thai *et al.*'s method) achieves the maximum accuracy of 99.79%. However, their performance declines sharply to an unacceptable level for enhanced images. In contrast, the proposed method can achieve competitive performance on original images and outperform the compared methods on enhanced images by a remarkable margin.

VI. CONCLUSION

Forensic analysis of JPEG-domain enhancement is challenging due to the difficulty in characterizing the mixed artifacts caused by JPEG compression and enhancement. This work addresses this challenge to some extent by proposing a novel likelihood function to characterize the mixed artifacts from the perspective of DCT coefficient periodicity. Based on the proposed likelihood function, a forensic method of enhancement detection and parameter estimation is developed for two classical methods of JPEG-domain enhancement. The encouraging performance under various experimental settings has demonstrated the effectiveness of the proposed likelihood function and the developed forensic method.

In addition to JPEG-domain enhancement, some JPEG-domain as well as pixel-domain operations might cause mixed artifacts when they are adopted to process JPEG images. Their forensic analysis also faces the challenge of effectively characterizing the mixed artifacts. The idea behind the proposed likelihood function might provide some inspiration for the forensic analysis of these operations.

The effectiveness of the proposed method is attributed to the good likelihood modeling of JPEG coefficients. It might not be suitable to forensically analyze some state-of-the-art enhancement methods that are not JPEG-coefficient based. To better deploy the proposed method, forensics analysts can first use the existing learning-based methods to roughly identify what type of operation an image has undergone, and then feed the image to the proposed method for secondary detection and parameter estimation if it is identified to be JPEG-domain enhanced. In such a way, the proposed method helps to not only confirm the identification result, but also provide more accurate parameter information for higher-level analysis.

REFERENCES

[1] A. Rocha, W. Scheirer, T. Boult, and S. Goldenstein, "Vision of the unseen: Current trends and challenges in digital image and video forensics," *ACM Comput. Surv.*, vol. 43, no. 4, pp. 1–42, Oct. 2011.

[2] A. Piva, "An overview on image forensics," *ISRN Signal Process.*, vol. 2013, Jan. 2013, Art. no. 496701.

[3] A. C. Popescu and H. Farid, "Exposing digital forgeries by detecting traces of resampling," *IEEE Trans. Signal Process.*, vol. 53, no. 2, pp. 758–767, Feb. 2005.

[4] T. Qiao, R. Shi, X. Luo, M. Xu, N. Zheng, and Y. Wu, "Statistical model-based detector via texture weight map: Application in re-sampling authentication," *IEEE Trans. Multimedia*, vol. 21, no. 5, pp. 1077–1092, May 2019.

[5] X. Liu, W. Lu, Q. Zhang, J. Huang, and Y.-Q. Shi, "Downscaling factor estimation on pre-JPEG compressed images," *IEEE Trans. Circuits Syst. Video Technol.*, vol. 30, no. 3, pp. 618–631, Mar. 2020.

[6] X. Kang, M. C. Stamm, A. Peng, and K. J. R. Liu, "Robust median filtering forensics using an autoregressive model," *IEEE Trans. Inf. Forensics Security*, vol. 8, no. 9, pp. 1456–1468, Sep. 2013.

[7] C. Pasquini, G. Boato, N. Alajlan, and F. G. B. De Natale, "A deterministic approach to detect median filtering in 1D data," *IEEE Trans. Inf. Forensics Security*, vol. 11, no. 7, pp. 1425–1437, Jul. 2016.

[8] G. Cao, Y. Zhao, R. Ni, and X. Li, "Contrast enhancement-based forensics in digital images," *IEEE Trans. Inf. Forensics Security*, vol. 9, no. 3, pp. 515–525, Mar. 2014.

[9] C. Chen, J. Ni, Z. Shen, and Y. Q. Shi, "Blind forensics of successive geometric transformations in digital images using spectral method: Theory and applications," *IEEE Trans. Image Process.*, vol. 26, no. 6, pp. 2811–2824, Jun. 2017.

[10] Q. Liu, "An improved approach to exposing JPEG seam carving under recompression," *IEEE Trans. Circuits Syst. Video Technol.*, vol. 29, no. 7, pp. 1907–1918, Jul. 2019.

[11] H. Li, W. Luo, and J. Huang, "Localization of diffusion-based inpainting in digital images," *IEEE Trans. Inf. Forensics Security*, vol. 12, no. 12, pp. 3050–3064, Dec. 2017.

[12] J. Fridrich, M. Goljan, and R. Du, "Steganalysis based on JPEG compatibility," *Proc. SPIE*, vol. 4518, pp. 275–280, Nov. 2001.

[13] Z. Fan and R. L. de Queiroz, "Identification of bitmap compression history: JPEG detection and quantizer estimation," *IEEE Trans. Image Process.*, vol. 12, no. 2, pp. 230–235, Feb. 2003.

[14] R. Neelamani, R. de Queiroz, Z. Fan, S. Dash, and R. G. Baraniuk, "JPEG compression history estimation for color images," *IEEE Trans. Image Process.*, vol. 15, no. 6, pp. 1365–1378, Jun. 2006.

[15] S. Ye, Q. Sun, and E.-C. Chang, "Detecting digital image forgeries by measuring inconsistencies of blocking artifact," in *Proc. IEEE Multimedia Expo Int. Conf.*, Jul. 2007, pp. 12–15.

[16] W. Luo, J. Huang, and G. Qiu, "JPEG error analysis and its applications to digital image forensics," *IEEE Trans. Inf. Forensics Security*, vol. 5, no. 3, pp. 480–491, Sep. 2010.

[17] G.-S. Lin, M.-K. Chang, and Y.-L. Chen, "A passive-blind forgery detection scheme based on content-adaptive quantization table estimation," *IEEE Trans. Circuits Syst. Video Technol.*, vol. 21, no. 4, pp. 421–434, Apr. 2011.

[18] B. Li, T.-T. Ng, X. Li, S. Tan, and J. Huang, "Statistical model of JPEG noises and its application in quantization step estimation," *IEEE Trans. Image Process.*, vol. 24, no. 5, pp. 1471–1484, May 2015.

[19] T. H. Thai, R. Cogranne, F. Retraint, and T.-N.-C. Doan, "JPEG quantization step estimation and its applications to digital image forensics," *IEEE Trans. Inf. Forensics Security*, vol. 12, no. 1, pp. 123–133, Jan. 2017.

[20] J. Yang, Y. Zhang, G. Zhu, and S. Kwong, "A clustering-based framework for improving the performance of JPEG quantization step estimation," *IEEE Trans. Circuits Syst. Video Technol.*, vol. 31, no. 4, pp. 1661–1672, Apr. 2020.

[21] T. Bianchi and A. Piva, "Detection of nonaligned double JPEG compression based on integer periodicity maps," *IEEE Trans. Inf. Forensics Security*, vol. 7, no. 2, pp. 842–848, Apr. 2012.

[22] J. Yang, J. Xie, G. Zhu, S. Kwong, and Y.-Q. Shi, "An effective method for detecting double JPEG compression with the same quantization matrix," *IEEE Trans. Inf. Forensics Security*, vol. 9, no. 11, pp. 1933–1942, Nov. 2014.

[23] C. Deng, Z. Li, X. Gao, and D. Tao, "Deep multi-scale discriminative networks for double JPEG compression forensics," *ACM Trans. Intell. Syst. Technol.*, vol. 10, no. 2, pp. 1–20, Feb. 2019.

[24] J. Wang, H. Wanga, J. Li, X. Luo, Y.-Q. Shi, and S. K. Jha, "Detecting double JPEG compressed color images with the same quantization matrix in spherical coordinates," *IEEE Trans. Circuits Syst. Video Technol.*, vol. 30, no. 8, pp. 2736–2749, Aug. 2020.

[25] C. Pasquini, G. Boato, and F. Perez-Gonzalez, "Multiple JPEG compression detection by means of benford-Fourier coefficients," in *Proc. IEEE Int. Workshop Inf. Forensics Secur. (WIFS)*, Dec. 2014, pp. 113–118.

[26] S. Mandelli, N. Bonettini, P. Bestagini, V. Lipari, and S. Tubaro, "Multiple JPEG compression detection through task-driven non-negative matrix factorization," in *Proc. IEEE Int. Conf. Acoust., Speech Signal Process. (ICASSP)*, Apr. 2018, pp. 2106–2110.

[27] V. Verma, N. Agarwal, and N. Khanna, "DCT-domain deep convolutional neural networks for multiple JPEG compression classification," *Signal Process., Image Commun.*, vol. 67, pp. 22–33, Sep. 2018.

[28] S. Aghagolzadeh and O. K. Ersoy, "Transform image enhancement," *Opt. Eng.*, vol. 31, no. 3, pp. 614–627, 1992.

[29] K. Konstantinides, V. Bhaskaran, and G. Beretta, "Image sharpening in the JPEG domain," *IEEE Trans. Image Process.*, vol. 8, no. 6, pp. 874–878, Jun. 1999.

[30] J. Tang, J. Kim, and E. Peli, "Image enhancement in the JPEG domain for people with vision impairment," *IEEE Trans. Biomed. Eng.*, vol. 51, no. 11, pp. 2013–2023, Nov. 2004.

[31] J. Tang, E. Peli, and S. Acton, "Image enhancement using a contrast measure in the compressed domain," *IEEE Signal Process. Lett.*, vol. 10, no. 10, pp. 289–292, Oct. 2003.

[32] S. Lee, "An efficient content-based image enhancement in the compressed domain using retinex theory," *IEEE Trans. Circuits Syst. Video Technol.*, vol. 17, no. 2, pp. 199–213, Feb. 2007.

[33] J. Mukherjee and S. K. Mitra, "Enhancement of color images by scaling the DCT coefficients," *IEEE Trans. Image Process.*, vol. 17, no. 10, pp. 1783–1794, Oct. 2008.

[34] C.-M. Kuo, N.-C. Yang, C.-S. Liu, P.-Y. Tseng, and C.-K. Chang, "An effective and flexible image enhancement algorithm in compressed domain," *Multimedia Tools Appl.*, vol. 75, no. 2, pp. 1177–1200, Jan. 2016.

[35] W. Park, B. Lee, and M. Kim, "Fast computation of integer DCT-V, DCT-VIII, and DST-VII for video coding," *IEEE Trans. Image Process.*, vol. 28, no. 12, pp. 5839–5851, Dec. 2019.

[36] D. Mukherjee and S. Mukhopadhyay, "Hardware efficient architecture for 2D DCT and IDCT using Taylor-series expansion of trigonometric functions," *IEEE Trans. Circuits Syst. Video Technol.*, vol. 30, no. 8, pp. 2723–2735, Aug. 2020.

[37] Y. Li *et al.*, "Improved low-power cost-effective DCT implementation based on Markov random field and stochastic logic," *IEEE Trans. Circuits Syst. Video Technol.*, vol. 30, no. 10, pp. 3803–3813, Oct. 2020.

[38] C. Yim, "An efficient method for DCT-domain separable symmetric 2-D linear filtering," *IEEE Trans. Circuits Syst. Video Technol.*, vol. 14, no. 4, pp. 517–521, Apr. 2004.

[39] K.-W. Hung and W.-C. Siu, "Novel DCT-based image up-sampling using learning-based adaptive K-NN MMSE estimation," *IEEE Trans. Circuits Syst. Video Technol.*, vol. 24, no. 12, pp. 2018–2033, Dec. 2014.

[40] S.-H. Bae and M. Kim, "DCT-QM: A DCT-based quality degradation metric for image quality optimization problems," *IEEE Trans. Image Process.*, vol. 25, no. 10, pp. 4916–4930, Oct. 2016.
[41] G. Schaefer and M. Stich, "UCID: An uncompressed color image database," *Proc. SPIE*, vol. 5307, pp. 472–480, Dec. 2004.
[42] F. Ding, G. Zhu, J. Yang, J. Xie, and Y.-Q. Shi, "Edge perpendicular binary coding for USM sharpening detection," *IEEE Signal Process. Lett.*, vol. 22, no. 3, pp. 327–331, Mar. 2015.
[43] H. Li, W. Luo, X. Qiu, and J. Huang, "Identification of various image operations using residual-based features," *IEEE Trans. Circuits Syst. Video Technol.*, vol. 28, no. 1, pp. 31–45, Jan. 2018.
[44] B. Li, Z. Li, S. Zhou, S. Tan, and X. Zhang, "New steganalytic features for spatial image steganography based on derivative filters and threshold LBP operator," *IEEE Trans. Inf. Forensics Security*, vol. 13, no. 5, pp. 1242–1257, May 2018.
[45] J. Kodovsky, J. Fridrich, and V. Holub, "Ensemble classifiers for steganalysis of digital media," *IEEE Trans. Inf. Forensics Security*, vol. 7, no. 2, pp. 432–444, Apr. 2012.

Jianquan Yang received the B.S. degree in communication engineering and the M.S. degree in communication and information system from Sun Yat-sen University, Guangzhou, China, in 2008 and 2010, respectively. He is currently pursuing the Ph.D. degree with the Shenzhen College of Advanced Technology, University of Chinese Academy of Sciences. He is currently an Assistant Professor with the Shenzhen Institute of Advanced Technology, Chinese Academy of Sciences, China. His research interests include multimedia security and pattern recognition.

Guopu Zhu (Senior Member, IEEE) received the B.S. degree in transportation from Jilin University, China, in 2002, and the M.S. and Ph.D. degrees in control science and engineering from the Harbin Institute of Technology, China, in 2004 and 2007, respectively. He was a Post-Doctoral Fellow with Sun Yat-sen University, Guangzhou, China, and a Senior Research Associate with the City University of Hong Kong, Hong Kong. He is currently a Professor with the Shenzhen Institute of Advanced Technology, Chinese Academy of Sciences, China, where he is the Director of the Center for Internet of Things Computing. He has authored or co-authored more than 40 articles in peer-reviewed international journals. His main research interests include multimedia security, image processing, and control theory. He serves as an Associate Editors for *IET Electronics Letters* and *Journal of Information Security and Applications*.

Yao Luo received the B.S. degree in electronic science and technology and the M.S. degree in physics and electronics from Yunnan University, China, in 2013 and 2016, respectively. She was a Visiting Student with the Shenzhen Institute of Advanced Technology, Chinese Academy of Sciences, China. She is currently a Software Engineer with Accuray Inc. Her research interests include image processing and multimedia security.

Sam Kwong (Fellow, IEEE) received the B.Sc. degree in electrical engineering from the State University of New York, Buffalo, NY, USA, in 1983, the M.Sc. degree in electrical engineering from the University of Waterloo, Waterloo, ON, Canada, in 1985, and the Ph.D. degree from the University of Hagen, Germany, in 1996. From 1985 to 1987, he was a Diagnostic Engineer with the Control Data Canada, Mississauga, ON, Canada. He later joined Bell Northern Research Canada, Ottawa, ON, Canada, as a member of Scientific Staff, and the City University of Hong Kong (CityU), Hong Kong, as a Lecturer with the Department of Electronic Engineering in 1990. He is currently a Chair Professor with the Department of Computer Science, CityU. His research interests include video coding, pattern recognition, and evolutionary algorithms. He is currently the Vice-President of Cybernetics with the IEEE TRANSACTIONS ON SYSTEMS, MAN AND CYBERNETICS. He also serves as an Associate Editor for the IEEE TRANSACTIONS ON EVOLUTIONARY COMPUTATION, the IEEE TRANSACTIONS ON INDUSTRIAL ELECTRONICS, and the IEEE TRANSACTIONS ON INDUSTRIAL.

Xinpeng Zhang (Member, IEEE) received the B.S. degree in computational mathematics from Jilin University, China, in 1995, and the M.E. and Ph.D. degrees in communication and information system from Shanghai University, China, in 2001 and 2004, respectively. Since 2004, he has been a Faculty Member with the School of Communication and Information Engineering, Shanghai University, where he is currently a Professor. He is also a Faculty Member with the School of Computer Science, Fudan University. He was with The State University of New York at Binghamton, as a Visiting Scholar, from 2010 to 2011, and Konstanz University as an experienced Researcher, sponsored by the Alexander von Humboldt Foundation, from 2011 to 2012. His research interests include multimedia security, AI security, and image processing. He has published over 300 articles in these areas. He was an Associate Editor of the IEEE TRANSACTIONS ON INFORMATION FORENSICS AND SECURITY from 2014 to 2017.

Yicong Zhou (Senior Member, IEEE) received the B.S. degree in electrical engineering from Hunan University, Changsha, China, and the M.S. and Ph.D. degrees in electrical engineering from Tufts University, Medford, MA, USA.

He is currently an Associate Professor and the Director of the Vision and Image Processing Laboratory, Department of Computer and Information Science, University of Macau, Macau. His research interests include image processing, computer vision, machine learning, and multimedia security.

Dr. Zhou is a fellow of the Society of Photo-Optical Instrumentation Engineers (SPIE). He received the Third Price of Macao Natural Science Award as a sole winner in 2020 and a co-recipient in 2014. He was also a recipient of the Best Editor Award for his contributions to *Journal of Visual Communication and Image Representation* in 2020. He has been a leading Co-Chair of Technical Committee on Cognitive Computing in the IEEE Systems, Man, and Cybernetics Society since 2015. He serves as an Associate Editor for IEEE TRANSACTIONS ON NEUTRAL NETWORKS AND LEARNING SYSTEMS, IEEE TRANSACTIONS ON CIRCUITS AND SYSTEMS FOR VIDEO TECHNOLOGY, IEEE TRANSACTIONS ON GEOSCIENCE AND REMOTE SENSING, and four other journals. He was recognized as the "Highly Cited Researcher" in Web of Science in 2020.